Design, Synthesis, and Characterization of Bent-Core Mesogen-Jacketed Liquid Crystalline Polymers

Xiaofang Chen,[†,‡] Kishore K. Tenneti,[‡] Christopher Y. Li,[*,‡] Yaowen Bai,[†] Rong Zhou,[†] Xinhua Wan,[†] Xinghe Fan,[†] and Qi-Feng Zhou[*,†]

Department of Polymer Science and Engineering and The Key Laboratory of Polymer Chemistry and Physics of Ministry of Education, College of Chemistry, Peking University, Beijing 100871, People's Republic of China, and A. J. Drexel Nanotechnology Institute and Department of Materials Science and Engineering, Drexel University, Philadelphia, Pennsylvania 19104

Received September 5, 2005; Revised Manuscript Received November 11, 2005

ABSTRACT: We report the design, synthesis, and characterization of a series of mesogen-jacketed liquid crystalline polymers with bent-core liquid crystals (BCLCs). For the first time, BCLC mesogens were directly side-attached to the polymer backbone and bent-core mesogen-jacketed liquid crystalline polymers (BMJLCPs) were achieved. Both three-ring and five-ring mesogens were employed. The *n*-alkoxy substituent lengths for the three-ring and five-ring BMJLCPs were controlled as $n = 1-5$ and $n = 6-16$, respectively. Various characterization techniques such as differential scanning calorimetry, wide-angle X-ray diffraction, and polarized light microscopy were used to study their mesomorphic phase behavior. The monomers of five-ring BMJLCPs with relatively long tails showed mesophase behavior. Columnar liquid crystalline phase was observed in both three-ring and five-ring BMJLCPs. Columnar rectangular (Φ_R) phase was observed in the three-ring system. In the five-ring BMJLCPs, relatively short-tail homologues possess Φ_R phase, while columnar hexagonal phase was observed in the long-tail samples. The differences in the phase structures were attributed to the "softness" of the macromolecular BMJLCP column surface.

Introduction

Rigid polymer chains are both structurally unique and technologically important compared to their random coil counterparts. Macromolecular chain rigidity can be induced by helical chain conformation (e.g. polypeptides) as well as aromatic backbones (e.g. polyimides). Side groups also have profound effects on main chain conformation. Large side groups can induce relatively extended chain conformation, which leads to liquid crystalline (LC) phase behavior (also known as enthalpy- driven mesophase formation).[1] One typical example is mesogen-jacketed liquid crystalline polymers (MJLCPs), proposed by Zhou et al.[2,3] In this system, mesogenic units are laterally attached to the backbone. As evidenced by small-angle neutron scattering (SANS) technique,[4,5] strong interaction between the polymer backbone and the mesogen groups leads to rigid chain conformation as well as liquid crystallinity. Several series of MJLCPs have been synthesized by a number of research groups, including poly{2,5-bis[(4-alkoxybenzoyl)oxy]-styrene},[6,7] poly[2,5-bis(4-alkoxybenzamido)styrene],[8] poly{2,5-bis[(4-alkoxyphenyl)oxycarbonyl]styrene},[9] and poly[2,5-bis(4′-alkoxyphenyl)styrene].[10] In all these polymers, the flexible backbones adopt a nearly extended conformation and the side groups wrap around the main chain; macromolecular columns are thus formed. LC columnar nematic phase (Φ_N) is the most often observed phase in MJLCPs, in which, the macromolecular columns, instead of individual molecular mesogens, possess the LC orientational order.[11,12] Higher ordered LC phases, such as columnar hexatic phase (Φ_{Hex}) and columnar hexagonal phase (Φ_H) have also been reported.[12−14] Phase behavior of MJLCPs depends on polymer molecular weight (MW), which was demonstrated by using monodispersed polymers prepared by controlled free radical polymerization techniques.[10] Both nitroxide-mediated radical polymerization[7,15] and atom-transfer radical polymerization have been employed.[16] Φ_N and Φ_{Hex} phases were found in poly{2,5-bis[(4-methoxyphenyl)oxycarbonyl]styrene} (PMPCS) with relatively low and high MW, respectively.[12] In laterally attached LC polymer systems *with* spacers, the nematic (N) phase is the most frequently observed phase. Lecommandux et al. observed N and smectic C (SmC) polymorphisms in the side-on LCPs with polysiloxane backbone.[17,18] Using SANS, they demonstrated that, for samples with a short spacer and aliphatic tails, the polymer chain was strongly stretched. Smectic A (SmA) and SmC phases have also been found in laterally attached side-chain LC polynorbornenes,[19−23] while Percec et al. reported columnar phases in monodendron-jacketed polymer systems, when bulky dendron-like side chains were attached to the flexible backbone.[24−26]

From a self-assembly point of view, the macromolecular columns/rods formed by MJLCPs can be used to create rod−coil molecular architechture.[27−32] Unique structures and morphologies have been observed in rod−coil molecules.[11,32−35] Rod structure control is pivotal to the self-assembly behavior of rod−coil molecules. The structure parameters of the rods include their length, diameter, and the surface chemistry. In the rigid rods induced by helical polymer chains or aromatic backbones, the rod length can be readily controlled by tuning MW. However, other parameters such as the rod diameter, surface chemistry of the rods can*not* be easily controlled. To this end, MJLCP is attractive due to the structural tunability that it can offer: rod length can be controlled by the MW of the MJLCPs, and, since the mesogens are oblique to the rod axes,[11,12] rod diameter can be controlled by tuning both the mesogen and tail lengths of the LC side chains. Furthermore, in all of the previously reported MJLCP work, linear LC mesogens (2,5

* To whom correspondence should be addressed. Phone: 215-895-2083 (C.Y.L.); 86-62756660 (Q.-F.Z.). Fax: 215-895-6760 (C.Y.L.). E-mail: chrisli@drexel.edu (C.Y.L.); qfzhou@pku.edu.cn (Q.-F.Z.).
† Peking University.
‡ Drexel University.

10.1021/ma051939d CCC: $33.50
Published on Web 12/24/2005

Scheme 1. Mesogen-Jacketed Liquid Crystalline Polymers (MJLCPs) with Linear and Bent-Core Liquid Crystalline (LC) Mesogens[a]

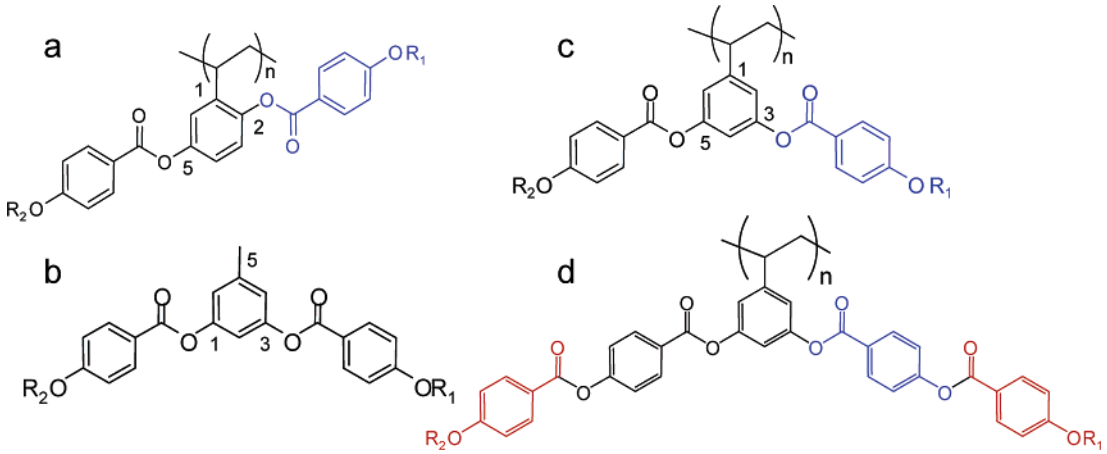

[a] Panel a shows the MJLCP with 2,5-substituted, linear jacketing mesogen; b shows the structure of a bent-core liquid crystal; c is bent-core mesogen-jacketed liquid crystalline polymers with a 3,5-substituted, bent-jacketing three-ring mesogen (the only difference between a and c is the substituting positions of the central core); d shows the 3,5-substituted, bent-jacketing five-ring mesogen. Relatively large mesogens led to a more significant jacketing effect.

substitution of the central ring) were used as shown in Scheme 1a. The ortho position of the backbone renders a tight "wrapping" effect to the MJLCP. We anticipate that the substitution position will have a dramatic effect on the rod formation in MJLCP systems. If 3,5 positions of the central ring are used to form a LC mesogen (Scheme 1c), bent-core LCs (BCLCs) will be achieved and the substitution position effect on the MJLCP LC phase formation can thus be tested.

BCLC itself is of great interest. In the small-mass LC research field, as a unique type of LC mesogens, BCLCs have attracted much attention in recent years due to their spectacular structure/properties. Although first synthesized as early as in 1923,[36] BCLCs, also known as banana liquid crystals due to their bent shape, were considered as "bad rods" until their intriguing phase and electrooptic properties were reported in 1996.[37−39] Seven novel *banana* LC phases have been observed, and they are named as B1−B7 (B stands for banana). Astonishing LC structures have been observed. BCLC molecules also possess a strong dipole moment perpendicular to the end-to-end molecular direction (**n**).[40] This dipole moment can be easily aligned by electric field. Both ferroelectric (F) and antiferroelectric (AF) properties have also been observed.[41−44] Although tremendous research was conducted on small-mass BCLC phase structures, research on LC polymers containing BCLC mesogens is still limited. Side-chain BCLC polymers with polysiloxane backbone have been reported showing F switching behavior.[45] BCLC networks have recently been achieved.[46,47] In this paper, we report the design, synthesis, and characterization of a series of BCLC MJLCPs with different alkoxy tails. For the first time, BCLC mesogens were directly side-attached to polymer backbone and bent-core mesogen-jacketed LC polymers (BMJLCPs) were achieved. The monomers of BMJLCPs with relatively long tails showed mesophase behavior. Both BMJLCPs with three rings and five rings were investigated, and two LC columnar phases were synthesized. We envisage that the unique BMJLCP rod structure could be employed in molecular structure design and a variety of rod−coil systems with tunable rod structures could be achieved.

Experimental Section

Materials. Orcinol (98%), 4-(dimethylamino)pyridine (DMAP, 99%), and triphenylphosphine (99%) were used as received from Acros. 4-Methyloxybenzoic acid (98%), 4-ethyloxybenzoic acid (98%), 4-propoxybenzoic acid (98%), 4-butyloxybenzoic acid (98%), 4-pentyloxybenzoic acid (98%), 4-hexyloxybenzoic acid (98%), and *N*-bromosuccinimide (NBS, 99%) were used as received from Aldrich. *p*-Hydroxybenzoic acid (99%,), methyl chloroformate (96%), bromooctane (98%), bromodecane (98%), bromododecane (98%), bromotetradecane (98%), bromohexadecane (98%), *N*,*N*′-dicyclohexylcarbodiimide (DCC, 95%) and 40% formaldehyde aqueous solution were used as received from Beijing Chemical Co. Other 4-alkoxybenzoic acids ($n > 6$) were prepared by etherification of 4-hydroxybenzoic acid with corresponding alkyl bromide and followed by recrystallization before use. 5-Methyl-1,3-phenylene bis(4-alkoxy)benzoate (T-MeCn) were obtained by esterification of orcinol with appropriate 4-alkoxybenzoic acid using the carbodiimide method. 5-Methyl-1,3-phenylenebis(4-hydroxy)benzoate was prepared according to the literature.[48] Azobisisobutyronitrile (AIBN) was recrystallized from ethanol before use. Benzoyl peroxide (BPO) was recrystallized from chloroform and methanol. Tetrahydrofuran (THF) was refluxed over sodium under argon and distilled out before use. Chlorobenzene was dried by distilling from CaH_2 under argon atmosphere. Other solvents and reagents were purchased from Beijing Chemical and used as received.

Synthesis of Precursors and Monomers. Parts a and b of Scheme 2 show the synthetic route for the monomers of the three- and five-ring BMJLCPs.

(A) Synthesis of the Three-Ring BCLC System, 5-Vinyl-1,3-phenylenebis(4-alkoxy)benzoate (T-VC*n*). The monomers were synthesized as in the following example of 5-vinyl-1,3-phenylene bis(4-methoxy)benzoate (T-VC1). 5-Methyl-1,3-phenylene bis(4-methoxy)benzoate (T-MeC1; 5.52 g, 0.014 mol), NBS (3.008 g, 0.0169 mol), BPO (67.8 mg, 0.0003 mol), and 200 mL of tetrachloromethane (CCl_4) were added to a round-bottom flask. The mixture was refluxed until the orange color faded. The precipitate was filtered off and washed with tetrachloromethane. After evaporation of solvent, the residue was boiled with 3.67 g (0.014 mol) of triphenylphosphine in 100 mL of xylene for 8 h. The obtained phosphonium salt was purified by silica gel column chromatography with dichloromethane and methanol as the eluent to yield 3.07 g (30%) of phosphonium salt yellow solid.

Monomer T-VC1 was obtained by Wittig reaction. A 19 mL aliquot of 0.5 M K_2CO_3 aqueous solution was slowly added to 60 mL of 40% formaldehyde containing 7 g of the above obtained phosphonium salt. The mixture was stirred for 24 h at room temperature. After extraction of the mixture with dichloromethane and evaporation of solvent, the resultant crude product was purified first by column chromatography (silica gel; dichloromethane/petroleum ether, 3/1) followed by recrystallization from ethanol/THF to yield 0.4 g of T-VC1 white solid (50%).

(1) T-VC1. ^{1}H NMR: δ 4.03−4.06 (t, 6H, -OC*H*$_3$), 5.33 (d, 1H, -CH=C*H*$_2$), 5.79 (d, 1H, -CH=C*H*$_2$), 6.70 (m, 1H, -C*H*=CH$_2$),

Scheme 2. Synthetic Route of the Monomers and Polymers of (a) the Three-Ring Series [T-MeC*n*, 5-Methyl-1,3-phenylenebis-[(4-alkoxy)benzoate]; T-VC*n*, 5-Vinyl-1,3-phenylenebis[(4-alkoxy)benzoate]; T-PVC*n*, Poly{(5-vinyl-1,3-phenylenebis-[(4-alkoxy)benzoate]}] and (b) the Five-Ring Series [F-MeC*n*, 5-Methyl-1,3-phenylenebis[4-(4′-alkoxybenzoyloxy)benzoate]]; F-VC*n*, 5-Vinyl-1,3-phenylenebis[4-(4′-alkoxybenzoyloxy)benzoate]; F-PVC*n*, Poly{5-vinyl-1,3-phenylenebis[4-(4′-alkoxybenzoyloxy)benzoate]}]

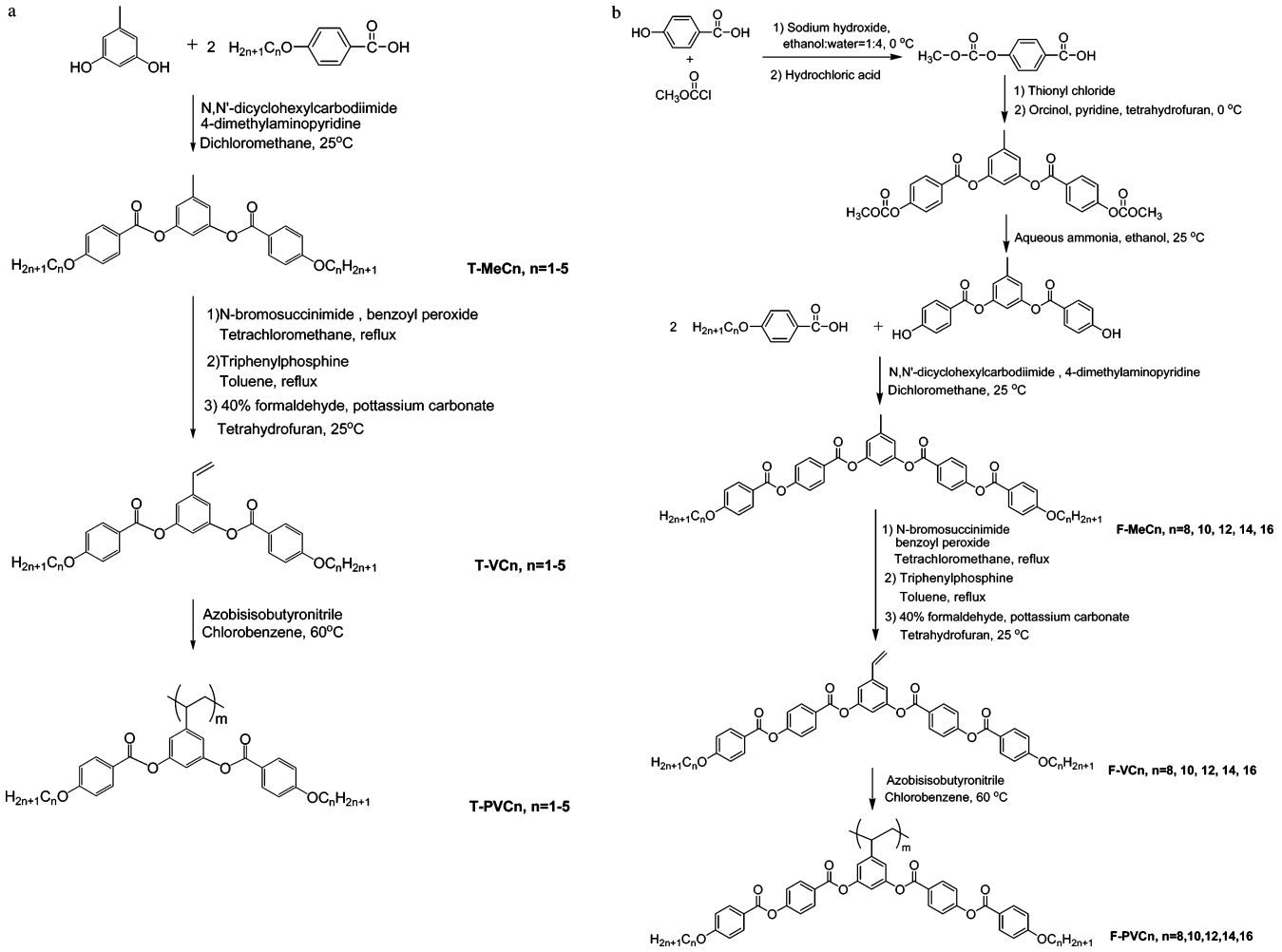

6.98−8.16 (m, 11H, Ar−H). Anal. Calcd for $C_{24}H_{20}O_6$: C, 71.28; H, 4.98. Found: C, 71.43; H, 4.86.

(2) T-VC2. ^{1}H NMR: δ 0.87−0.91 (t, 6H, -CH_3), 4.03−4.06 (t, 4H, -OCH_2-), 5.35 (d, 1H, -CH=CH_2), 5.81 (d, 1H, -CH=CH_2), 6.70 (m, 1H, -CH=CH$_2$), 6.98−8.16 (m, 11H, Ar−H). Anal. Calcd for $C_{26}H_{24}O_6$: C, 72.21; H, 5.59. Found: C, 72.41; H, 5.62.

(3) T-VC3. ^{1}H NMR: δ 0.87−0.91(t, 6H, -CH_3), 1.82−1.84 (m, 4H, -OCH$_2$CH_2-), 4.03−4.06 (t, 4H, -OCH_2-), 5.35(d, 1H, -CH=CH_2), 5.81 (d, 1H, -CH=CH_2), 6.70 (m, 1H, -CH=CH$_2$), 6.98−8.16 (m, 11H, Ar−H). Anal. Calcd for $C_{28}H_{28}O_6$: C, 73.03; H, 6.13. Found: C, 73.12; H, 6.10.

(4) T-VC4. ^{1}H NMR: δ 0.87−0.91(t, 6H, -CH_3), 1.21−1.59 (m, 4H, -CH_2CH$_3$), 1.82−1.84 (m, 4H, -OCH$_2$CH_2-), 4.03−4.06 (t, 4H, -OCH_2-), 5.35 (d, 1H, -CH=CH_2), 5.81 (d, 1H, -CH=CH_2), 6.70 (m, 1H, -CH=CH$_2$), 6.98−8.16 (m, 11H, Ar−H). Anal. Calcd for $C_{30}H_{32}O_6$: C, 73.75; H, 6.60. Found: C, 73.75; H, 6.60.

(5) T-VC5. ^{1}H NMR: δ 0.87−0.91 (t, 6H, -CH_3), 1.21−1.59 (m, 8H, -(CH_2)$_2$CH$_3$), 1.82−1.84 (m, 4H, -OCH$_2$CH_2-), 4.03−4.06 (t, 4H, -OCH_2-), 5.35 (d, 1H, -CH=CH_2), 5.81 (d, 1H, -CH=CH_2), 6.70 (m, 1H, -CH=CH$_2$), 6.98−8.16 (m, 11H, Ar−H). Anal. Calcd for $C_{32}H_{36}O_6$: C, 74.39; H, 7.02. Found: C, 74.58; H, 6.89.

(B) Synthesis of the Five-Ring BCLC System, 5-Vinyl-1,3-phenylenebis[4-(4′-alkoxybenzoyloxy)benzoate] (F-VC*n*). (1) 5-Methyl-1,3-phenylenebis[4-(4′-alkoxybenzoyloxy)benzoate] (F-MeC*n*). F-MeC*n*s were synthesized using the following procedure (n = 8 was used as the example). 5-Methyl-1,3-phenylenebis(4-hydroxy)benzoate (5.818 g, 0.016 mol), 4-octyloxybenzoic acid (11.320 g, 0.032 mol), DCC (8.395 g, 0.0474 mol), and DMAP (0.39 g, 0.003 mol) were dissolved in dichloromethane. The solution was stirred at room temperature for about 8 h. The precipitate was filtered and washed with dichloromethane for several times. After evaporation of the solvent, the obtained ester was purified by silica gel column chromatography with dichloromethane as the eluent to yield 11.9 g (90%) of F-MeC8.

(a) F-MeC8. ^{1}H NMR: δ 0.87−0.91(t, 6H, -CH_3), 1.29−1.36 (m, 20H, -(CH_2)$_5$CH$_3$), 1.82−1.84 (m, 4H, -OCH$_2$CH_2-), 2.36 (s, 3H, CH_3−Ar), 4.03−4.06 (t, 4H, -OCH_2-), 6.98−8.16 (m, 19H, Ar−H). Anal. Calcd for $C_{51}H_{56}O_{10}$: C, 73.89; H, 6.81. Found: C, 73.88; H, 6.82.

(b) F-MeC10. ^{1}H NMR: δ 0.87−0.91(t, 6H, -CH_3), 1.29−1.36 (m, 28H, -(CH_2)$_7$CH$_3$), 1.82−1.84 (m, 4H, -OCH$_2$CH_2-), 2.36 (s, 3H, CH_3−Ar), 4.03−4.06 (t, 4H, -OCH_2-), 6.98−8.16 (m, 19H, Ar−H). Anal. Calcd for $C_{55}H_{64}O_{10}$: C, 74.97; H, 7.19. Found: C, 74.62; H, 7.27.

(c) F-MeC12. ^{1}H NMR: δ 0.87−0.91(t, 6H, -CH_3), 1.29−1.36 (m, 36H, -(CH_2)$_9$CH$_3$), 1.82−1.84 (m, 4H, -OCH$_2$CH_2-), 2.36 (s, 3H, CH_3−Ar), 4.03−4.06 (t, 4H, -OCH_2-), 6.98−8.16 (m, 19H, Ar−H). Anal. Calcd for $C_{59}H_{72}O_{10}$: C, 75.29; H, 7.71. Found: C, 75.21; H, 7.68.

(d) F-MeC14. ^{1}H NMR: δ 0.87−0.91(t, 6H, -CH_3), 1.29−1.36-(m, 44H, -(CH_2)$_{11}$CH$_3$), 1.82−1.84 (m, 4H, -OCH$_2$CH_2-), 2.36 (s, 3H, CH_3−Ar), 4.03−4.06 (t, 4H, -OCH_2-), 6.98−8.16 (m, 19H, Ar−H). Anal. Calcd for $C_{63}H_{80}O_{10}$: C, 75.87; H, 8.09. Found: C, 75.76; H, 7.98.

(e) F-MeC16. ^{1}H NMR: δ 0.87−0.91 (t, 6H, -CH_3), 1.29−1.36 (m, 52H, -(CH_2)$_{13}$CH$_3$), 1.82−1.84 (m, 4H, -OCH$_2$CH_2-), 2.36 (s, 3H, CH_3−Ar), 4.03−4.06 (t, 4H, -OCH_2-), 6.98−8.16 (m, 19H,

Ar−H). Anal. Calcd for $C_{63}H_{80}O_{10}$: C, 76.39; H, 8.42. Found: C, 76.15; H, 8.44.

(2) 5-Vinyl-1,3-phenylenebis[4-(4′-alkoxybenzoyloxy)benzoate] (F-VC*n*). F-VC*n*s were synthesized as in the following example ($n = 8$). 5-Methyl-1,3-phenylenebis[4-(4′- octyloxybenzoyloxy)benzoate] (F-MeC8; 8.29 g, 0.010 mol), NBS (1.815 g, 0.0102 mol), BPO (48.4 mg, 0.0002 mol), and 200 mL of tetrachloromethane were added to a round-bottom flask. The mixture was refluxed until the orange color faded. The precipitate was filtered and washed with tetrachloromethane. After evaporation of solvent, the residue was boiled with triphenylphosphine (2.62 g, 0.01 mol) in 100 mL of xylene for 8 h. The obtained phosphonium salt was purified by silica gel column chromatography with dichloromethane and methanol as the eluent to yield 3.51 g (30%) of phosphonium salt yellow solid.

Monomer F-VC8 was obtained by Wittig reaction. A 6 mL aliquot of 0.5 M K_2CO_3 aqueous solution was slowly added to 37 mL of 40% formaldehyde containing 3.5 g of the above obtained phosphonium salt. The mixture was stirred for 24 h at room temperature. After extraction of the mixture with dichloromethane and evaporation of solvent, the resultant crude product was purified first by column chromatography (silica gel; dichloromethane/petroleum ether, 3:1) followed by recrystallization from ethanol/THF to yield 1.26 g (50%) of F-VC8.

(a) F-VC8. ^{1}H NMR: δ 0.87−0.91(t, 6H, -C*H*$_3$), 1.29−1.36 (m, 20H, -(C*H*$_2$)$_5$CH$_3$), 1.82−1.84 (m, 4H, -OCH$_2$C*H*$_2$-), 4.03−4.06 (t, 4H, -OC*H*$_2$-), 5.35 (d, 1H, -CH=C*H*$_2$), 5.81 (d, 1H, -CH=C*H*$_2$), 6.70 (m, 1H, -C*H*=CH$_2$), 6.98−8.16 (m, 19H, Ar−H). ^{13}C NMR: δ 14.05 (-CH$_2$*C*H$_3$), 22.62−3l.77 (-(*C*H$_2$)$_6$CH$_3$), 68.36 (*C*H$_2$OAr), 114.40 (aromatic C ortho to OCH$_2$), 114.92 (aromatic C para to CH=CH$_2$), 116.02 (CH=*C*H$_2$), 117.02 (aromatic C ortho to CH=CH$_2$), 120.93 (aromatic *C* para to OCH$_2$), 122.11 (aromatic C ortho to OC=O), 126.55 (aromatic *C* to C=O), 131.81 (aromatic C ortho to C=O), 132.38 (aromatic C meta to OCH$_2$), 135.34 (*C*H=CH$_2$), 140.08 (aromatic *C*−CH=CH$_2$), 151.49 (aromatic C meta to CH=CH$_2$), 155.49 (aromatic *C*−O−C=O), 163.82 (aromatic *C*−OCH$_2$), 164.04−164.24 (*C*=O). Anal. Calcd for $C_{52}H_{56}O_{10}$: C, 74.26; H, 6.71. Found: C, 73. 77; H, 6.61.

(b) F-VC10. ^{1}H NMR: δ 0.87−0.91(t, 6H, -C*H*$_3$), 1.29−1.36 (m, 28H, -(C*H*$_2$)$_7$CH$_3$), 1.82−1.84 (m, 4H, -OCH$_2$C*H*$_2$-), 4.03−4.06 (t, 4H, -OC*H*$_2$-), 5.35 (d, 1H, -CH=C*H*$_2$), 5.81 (d, 1H, -CH=C*H*$_2$), 6.70 (m, 1H, -C*H*=CH$_2$), 6.98−8.16 (m, 19H, Ar−H). ^{13}CNMR: δ 14.08 (-CH$_2$*C*H$_3$), 22.64−3l.86 (-(*C*H$_2$)$_8$CH$_3$), 68.34 (*C*H$_2$OAr), 114.38 (aromatic C ortho to OCH$_2$), 114.91 (aromatic C para to CH=CH$_2$), 116.02 (CH=*C*H$_2$), 117.01 (aromatic C ortho to CH=CH$_2$), 120.89 (aromatic *C* para to OCH$_2$), 122.10 (aromatic C ortho to OC=O), 126.52 (aromatic *C* to C=O), 131.80 (aromatic C ortho to C=O), 132.38 (aromatic C meta to OCH$_2$), 135.32 (*C*H=CH$_2$), 140.06 (aromatic *C*−CH=CH$_2$), 151.47 (aromatic C meta to CH=CH$_2$), 155.47 (aromatic *C*−O−C=O), 163.79 (aromatic *C*−OCH$_2$), 164.01−164.22 (*C*=O). Anal. Calcd for $C_{56}H_{64}O_{10}$: C, 74.97; H, 7.19. Found: C, 73.57; H, 7.16.

(c) F-VC12. ^{1}H NMR: δ 0.87−0.91 (t, 6H, -C*H*$_3$), 1.29−1.36 (m, 36H, -(C*H*$_2$)$_9$CH$_3$), 1.82−1.84 (m, 4H, -OCH$_2$C*H*$_2$-), 4.03−4.06 (t, 4H, -OC*H*$_2$-), 5.35 (d, 1H, -CH=C*H*$_2$), 5.81 (d, 1H, -CH=C*H*$_2$), 6.70 (m, 1H, -C*H*=CH$_2$), 6.98−8.16 (m, 19H, Ar−H). ^{13}C NMR: δ 14.09 (-CH$_2$*C*H$_3$), 22.66−3l.89 (-(*C*H$_2$)$_{10}$CH$_3$), 68.36 (*C*H$_2$OAr), 114.41 (aromatic C ortho to OCH$_2$), 164.21−164.01 (*C*=O), 114.92 (aromatic C para to CH=CH$_2$), 116.01 (CH=*C*H$_2$), 117.01 (aromatic C ortho to CH=CH$_2$), 120.93 (aromatic *C* para to OCH$_2$), 122.10 (aromatic C ortho to OC=O), 126.55 (aromatic *C* to C=O), 131.81 (aromatic C ortho to C=O), 132.40 (aromatic C meta to OCH$_2$), 135.35 (*C*H=CH$_2$), 140.07(aromatic *C*−CH=CH$_2$), 151.51 (aromatic C meta to CH$_3$), 155.50 (aromatic *C*−O−C=O), 163.81 (aromatic *C*−OCH$_2$), 164.01−164.21 (*C*=O). Anal. Calcd for $C_{60}H_{72}O_{10}$: C, 75.60; H, 7.61. Found: C, 75.77; H, 7.68.

(d) F-VC14. ^{1}H NMR: δ 0.87−0.91 (t, 6H, -C*H*$_3$), 1.29−1.36 (m, 44H, -(C*H*$_2$)$_{11}$CH$_3$), 1.82−1.84 (m, 4H, -OCH$_2$C*H*$_2$-), 4.03−4.06 (t, 4H, -OC*H*$_2$-), 5.35 (d, 1H, -CH=C*H*$_2$), 5.81 (d, 1H, -CH=C*H*$_2$), 6.70 (m, 1H, -C*H*=CH$_2$), 6.98−8.16 (m, 19H, Ar−H). ^{13}C NMR: δ 14.07 (-CH$_2$*C*H$_3$), 22.64−3l.88 (-(*C*H$_2$)$_{12}$CH$_3$), 68.35 (*C*H$_2$OAr), 114.38 (aromatic C ortho to OCH$_2$), 114.91 (aromatic C para to CH=CH$_2$), 116.01 (CH=*C*H$_2$), 117.01 (aromatic C ortho to CH=CH$_2$), 120.89 (aromatic *C* para to OCH$_2$), 122.10 (aromatic C ortho to OC=O), 126.53 (aromatic *C* to C=O), 131.81 (aromatic C ortho to C=O), 132.38 (aromatic C meta to OCH$_2$), 135.31 (*C*H=CH$_2$), 140.06 (aromatic *C*−CH=CH$_2$), 151.46 (aromatic C meta to CH=CH$_2$), 155.46 (aromatic *C*−O−C=O), 163.79 (aromatic *C*−OCH$_2$), 164.03−164.24 (*C*=O). Anal. Calcd for $C_{64}H_{80}O_{10}$: C, 76.16; H, 7.99. Found: C, 75.78; H, 7.86.

(e) F-VC16. ^{1}H NMR: δ 0.87−0.91(t, 6H, -C*H*$_3$), 1.29−1.36 (m, 52H, -(C*H*$_2$)$_{13}$CH$_3$), 1.82−1.84 (m, 4H, -OCH$_2$C*H*$_2$-), 4.03−4.06 (t, 4H, -OC*H*$_2$-), 5.35 (d, 1H, -CH=C*H*$_2$), 5.81 (d, 1H, -CH=C*H*$_2$), 6.70 (m, 1H, -C*H*=CH$_2$), 6.98−8.16 (m, 19H, Ar−H). ^{13}C NMR: δ 14.08 (-CH$_2$*C*H$_3$), 22.65−3l.89 (-(*C*H$_2$)$_{14}$CH$_3$), 68.34 (*C*H$_2$OAr), 114.38 (aromatic C ortho to OCH$_2$), 114.91 (aromatic C para to CH=CH$_2$), 116.01 (CH=*C*H$_2$), 117.01 (aromatic C ortho to CH=CH$_2$), 120.89 (aromatic *C* para to OCH$_2$), 122.10 (aromatic C ortho to OC=O), 126.53 (aromatic *C* to C=O), 131.80 (aromatic C ortho to C=O), 132.38 (aromatic C meta to OCH$_2$), 135.32 (*C*H=CH$_2$), 140.06 (aromatic *C*−CH=CH$_2$), 151.47 (aromatic C meta to CH=CH$_2$), 155.47 (aromatic *C*−O−C=O), 163.79 (aromatic *C*−OCH$_2$), 164.01−164.22 (*C*=O). Anal. Calcd for $C_{68}H_{88}O_{10}$: C, 76.66; H, 8.33. Found: C, 76.37; H, 8.12.

(3) Polymerization. All polymers were obtained by conventional solution radical polymerization. A typical polymerization procedure is summarized as the following. About 0.4 g of F-VC10, 27 μL of 0.05 M AIBN chlorobenzene solution, and 2 mL of chlorobenzene were transferred into a polymerization tube. After three freeze−pump−thaw cycles, the tube was sealed under vacuum. Polymerization was carried out at 60 °C for 24 h. The tube was then opened, and the reaction mixture was diluted with 10 mL of THF. After evaporation of the solvent, the products were purified using column chromatography with dichloromethane as the eluent in order to remove unreacted monomers. Polymers were obtained by precipitation in methanol followed by drying under vacuum at room temperature for 24 h. Yields and MW are listed in Table 1.

Table 1. Synthesis and Thermotropic Behavior of Poly[5-vinyl-1,3-phenylenebis(4-alkoxy)benzoate] (T-PVC*n*) and Poly{5-vinyl-1,3-phenylenebis[4-(4′-alkoxybenzoyloxy)benzoate]} (F-PVC*n*))

polymer[a]	yield[b] (%)	GPC[c] $M_n \times 10^{-4}$ [d]	GPC[c] M_w[e]/M_n	T_g [f] (°C)	T_d [g] (°C)
T-PVC1	83	poor solubility in THF		133	436
T-PVC2	91	15.9	1.82	121	438
T-PVC3	88	11.9	1.84	110	447
T-PVC4	86	18.4	1.58	92	447
T-PVC5	75	6.3	2.25	77	454
F-PVC6	78	poor solubility in THF		114	450
F- P VC8	82	23.2	1.43	119	447
F-PVC10	93	14.1	1.90	134	445
F-PVC12	90	14.9	1.62	134	445
F-PVC14	88	17.2	1.93	140	455
F-PVC16	92	18.4	1.88	125	442

[a] As defined in Scheme 2 a,b. [b] Polymerized in chlorobenzene at 60 °C for 24 h using azobisisobutyronitrile (AIBN)as initiator; [monomer]:[AIBN] = 300:1 (molar ratio). [c] Molecular weights and polydispersity were measured by GPC, using tetrahydrofuran as an eluent at 35 °C, polystyrene as the standard. [d] M_n, number average molecular weight. [e] M_w, weight average molecular weight. [f] T_g, glass transition temperature. Determined from the second-heating DSC curves, peak temperatures. [g] T_d, decomposition temperature. Inflection points of the thermogravimetry curve were used.

Equipment and Experiments. ^{1}H NMR (400 MHz) and ^{13}C NMR (100 MHz) spectra were recorded on a Bruker ARX400 spectrometer using deuterated chloroform ($CDCl_3$) as the solvent for monomers and deuterated dichloromethane (CD_2Cl_2) for polymers; the chemical shifts were referenced to tetramethylsilane. Elemental analyses were recorded on an Elementar Vario EL instrument. Gel permeation chromatographic (GPC) measurements were performed with a Waters 2410 refractive-index detector at 35 °C, and THF was used as the eluent at a flow rate of 1.0 mL/min. Three Waters Styragel columns with 10 μm bead size were

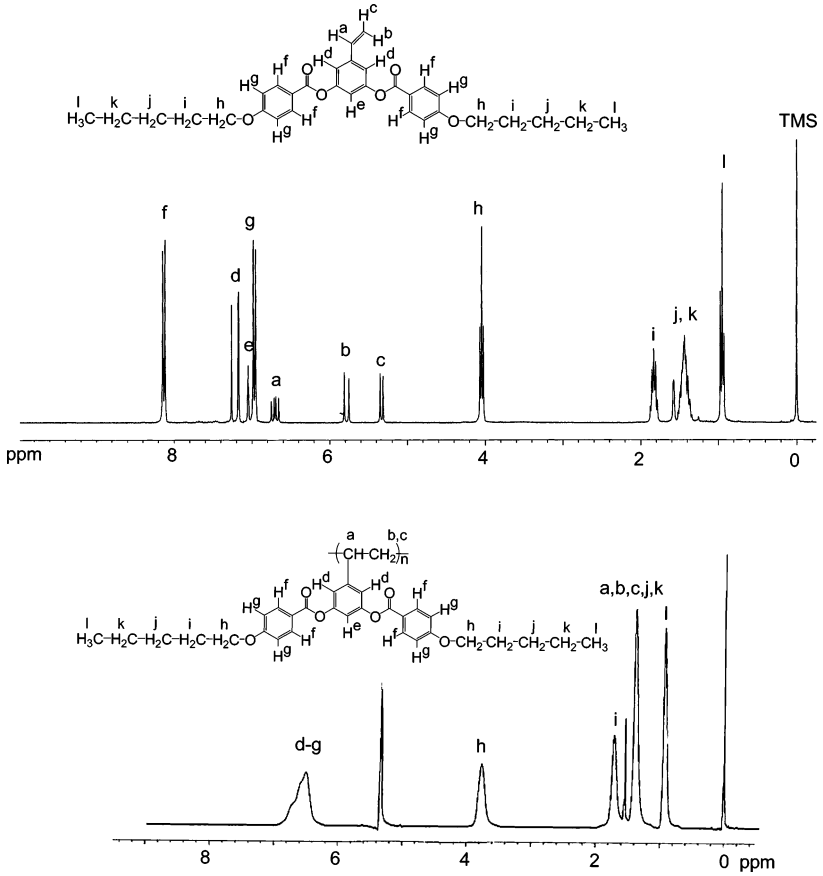

Figure 1. ^{1}H NMR spectra of 5-vinyl-1,3-phenylenebis[(4-pentyloxy)benzoate (T-VC5) and poly{(5-vinyl-1,3-phenylenebis[(4-pentyloxy)benzoate]} (T-PVC5) in $CDCl_3$ and CD_2Cl_2, respectively.

connected in series. Their effective molecular weight ranges were 100−10 000 for Styragel HT2, 500−30 000 for Styragel HT3, and 5000−600 000 for Styragel HT4, respectively. The pore sizes are 50, 100, and 1000 nm for Styragels HT2, HT3, and HT4, respectively. All GPC data were calibrated with polystyrene standards. The thermal transitions of the monomers and polymers were detected using Perkin-Elmer DSC-7 differential scanning calorimetry (DSC). The temperature and heat flow were calibrated using standard materials (indium and zinc) at different cooling and heating rates between 5 and 40 °C/min. Samples with a typical mass of 3−10 mg were encapsulated in sealed aluminum pans. A controlled cooling experiment was always carried out first, and a subsequent heating was performed at a rate that was equal to or faster than the previous cooling. The inflection point temperature was used to determine the glass transition temperature, and peak (endothermic maximum) temperature was used to determine the isotropization temperate of the liquid crystals. Thermogravimetric analyses (TGA) were performed on a Mettler-Toledo TGA/SDTA 851e instrument in nitrogen atmosphere using a heating rate of 20 °C/min. Wide-angle X-ray diffraction (WAXD) was carried out using a Philips X'Pert (Cu Kα, λ = 0.154 nm) with Anton Parr TTK 450 heating stage and Anton Parr TCU-100 thermal controller. Synchrotron beam lines X-18A and X-27C at Brookhaven National Laboratory were also used.

Two-dimensional WAXD patterns were recorded at room temperature for different exposure times using an imaging plate equipped with an 18 kW X-ray rotating anode generator (Cu Kα radiation, Rigaku automated X-ray imaging system with 1500 × 1500 pixel resolution). The air scattering was subtracted from the WAXD patterns. Polymer samples were hot-pressed at 200−250 °C between two glass slides, and the top slide was sheared at a rate ~ 1 Hz, leading to oriented polymer films with thickness ~ 0.1−0.2 mm.

LC texture was examined via a polarized light micrscope (PLM, Olympus BX-51) coupled with a Mettler-Toledo hot stage (FP 82 HT with a FP-90 central processor). The image was captured using an Insight digital camera. The film thickness was controlled to be ~10 μm, prepared by melt-pressing. The specimens were slightly sheared (shear rate ~ 1 Hz; shear amplitude ~ 20−50%) to increase the LC domain size.

Results and Discussion

Polymerization of BMJLCPs. Free radical polymerization of VC*n* initiated by AIBN in chlorobenzene gave the corresponding polymers, PVC*n*, with moderately high MW in good to excellent yields. The polymerization results are summarized in Table 1. PVC*n*s have good solubility in common organic solvents such as THF and chloroform.

Since the monomers have poor solubility in methanol, the normal precipitation process is not sufficient to remove unreacted monomers. Further purification was achieved by using column chromatography technique. The conversion and purification of polymers was confirmed by ^{1}H NMR spectroscopy and GPC. As an example, Figures 1 and 2 show the ^{1}H NMR spectra of monomers T-VC5 and F-VC10 and polymers T-PVC5 and F-PVC10. T-VC 5 and F-VC10 showed characteristic resonances of the vinyl group at 5.35−5.83 and 6.67−6.72 ppm (denoted as a, b, c in the figure), which completely disappeared after polymerization. The absorption peaks of T-PVC5 and F-PVC10 were quite broad and consistent with the expected polymer structure.

Mesomorphic Properties of VC*n* Monomers. The mesomorphic behavior of both three- and five-ring BCLC monomers was investigated using PLM, DSC, and WAXD methods. A mesophase was not observed in any of the three-ring T-VC*n* monomers. Compared to the LC PMPCS monomers, T-VC*n*s possess essentially the same chemical structure except for the

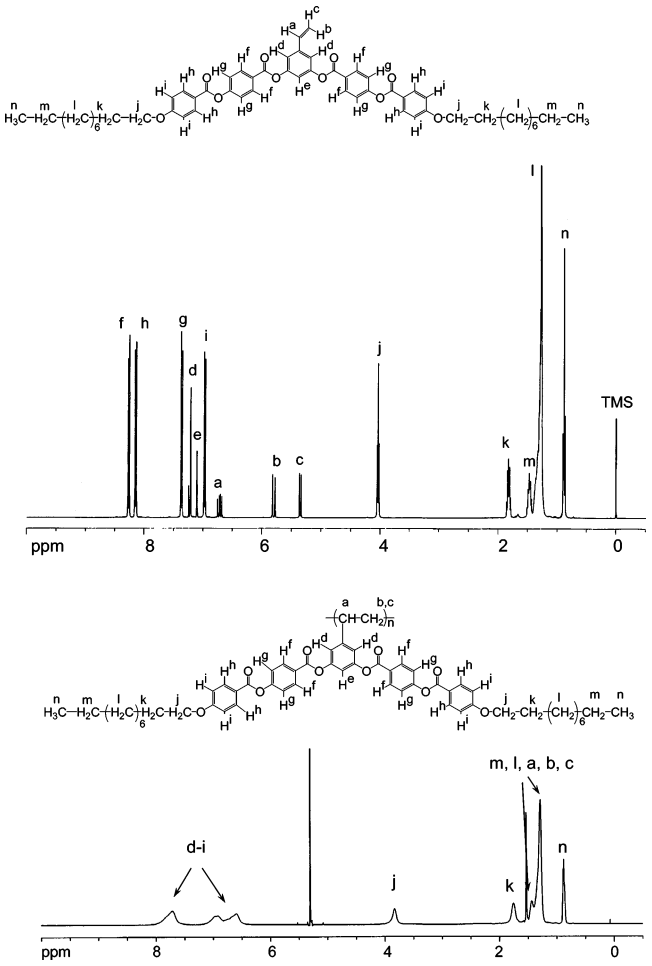

Figure 2. ^{1}H NMR spectra of 5-vinyl-1,3-phenylenebis[4-(4′-decyloxybenzoyloxy)benzoate] (F-VC10) and poly{5-vinyl-1,3-phenylenebis[4-(4′-decyloxybenzoyloxy)benzoate]} (F-PVC10) in $CDCl_3$ and CD_2Cl_2, respectively.

bent instead of linear mesogen.[10] A lack of liquid crystallinity in T-VC*n* indicates that linear mesogenic shape is essential for the LC phase formation for the three-ring system. However, unique LC phase behavior was reported in BCLCs with five (or higher number) benzene rings, indicating that a relatively longer mesogen is necessary to ensure the mesophase formation in BCLC systems.[43] Chemical substitution on the central benzene ring is also of critical importance for the BCLC phase behavior. It has been proposed that the substituting group at position 5 of bent molecules prevents the formation of a mesophase, since substitution groups attached at the central phenyl ring near the connecting groups strongly influence the bending angle between two arms and thus alter the stable molecular conformation. Until now, no mesophase has been found in five-ring bent-core compounds derived from 5-substituted resorcinol.[43,49] (Note that Reddy and Sadashiva reported the mesomorphic behavior of two homologous series of *seven-ring* compounds derived from 5-cyanoresorcinol).[50] In the five-ring system, liquid crystallinity was not observed in F-MeCn (methyl-substituted BCLC), which is consistent with the previously reported work.[43] Nevertheless, a mesophase *was* observed in the five-ring ester type compounds derived from 5-vinylresorcinol with relatively longer alkoxy tails F-VC*n* ($n = 14, 16$). Figure 3 shows DSC cooling and heating thermograms of F-VC14, -16 with a cooling/heating rate of 10 °C/min. Monotropic LC behavior is evident, which can be confirmed by PLM experiments. When cooling from isotropic phase, F-VC14

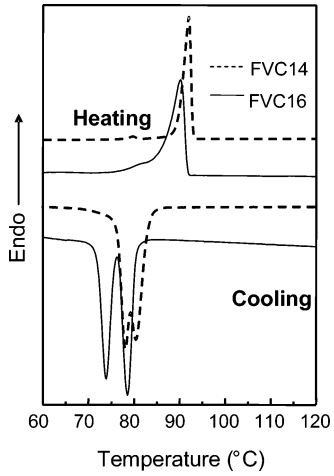

Figure 3. Differential scanning calorimetry curves of 5-vinyl-1,3-phenylenebis[4-(4′-tetradecyloxybenzoyloxy)benzoate] (F-VC14) and 5-vinyl-1,3-phenylenebis[4-(4′-hexadecyloxybenzoyloxy)benzoate] (F-VC16) at the rate of 10 °C/min.

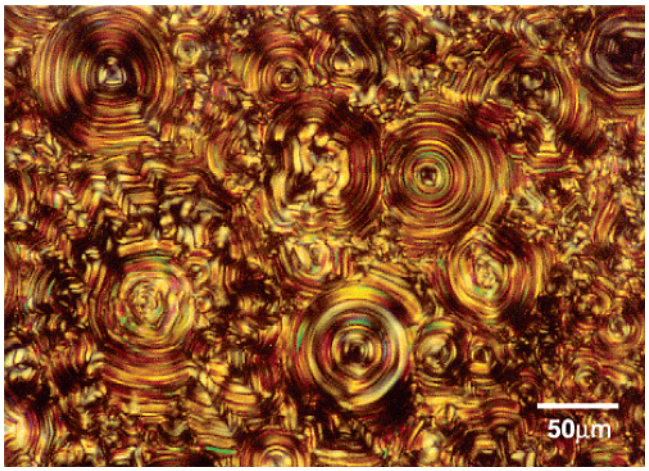

Figure 4. Polarized light microscope image of 5-vinyl-1,3-phenylenebis[4-(4′-tetradecyloxybenzoyloxy)benzoate] (F-VC14) developed from isotropic liquid at 70 °C.

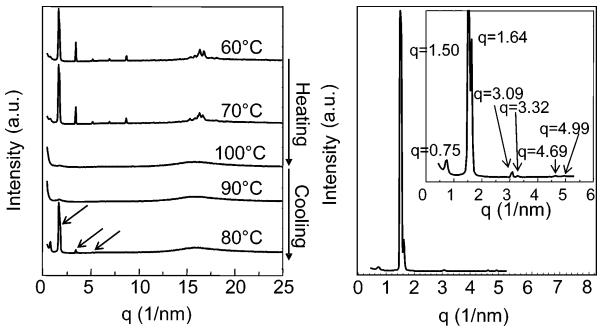

Figure 5. Powder wide-angle X-ray diffraction pattern of 5-vinyl-1,3-phenylenebis[4-(4′-tetradecyloxybenzoyloxy)benzoate] (F-VC14) heating/cooling at 10 °C/ min (a, left). Panel b (right) shows the enlarged diffraction curve of F-VC14 after cooling from isotropic to 80 °C. Bilayer as well as undulated structure can be clearly seen from the inset of b.

exhibits fringe-pattern domains, as shown in Figure 4. The thermal powder WAXD pattern of F-VC14 at different temperatures shows that, at room temperature, the crystalline phase was observed which directly transferred to isotropic melt upon heating. Upon cooling, the LC phase was formed before crystallization. Figure 5a shows the WAXD pattern of F-VC14 as a function of temperature. A broad scattering halo in the wide-

angle region can be clearly seen, indicating the liquidlike order of the molecules within the layers. Smectic layer structure is evident from the low-angle X-ray diffraction peaks shown in Figure 5b. Two distinct features can be seen from the diffraction pattern: (1) Doublet diffraction peaks at $q = 1.50$, 1.64; 3.09, 3.32; and 4.69, 4.99 nm^{-1} which can be assigned as smectic layers first, second, and third diffraction doublets. (2) There is a low intensity diffraction peak at $q_0 \sim 0.75$ nm^{-1} which is half of q_1 (1.50 nm^{-1}). The strong diffraction peak at $q = 1.50$ nm^{-1} indicates a layer spacing of 4.18 nm, which is smaller than the calculated molecular length L in the most extended form with all-trans conformation of the alkoxy chains and is close to the d spacing of SmCP phase formed by similar mesogens.[51] Observation of the doublets indicates the in-layer undulated structure formation, and using the $q = 1.50$ and 1.64 nm^{-1} as the (10) and (11) diffraction, a modulation wavelength of ~9.59 nm can be calculated.[52] Furthermore, since conventional instead of resonant XRD was used in the present study, observation of the low-angle weak diffraction at 0.75 nm^{-1} suggests a bilayer structure formation and the smectic phase might belong to a triclinic smectic CG phase (also known as the B7 phase).[53] Note that G stands for "generalized" as predicted by de Gennes.[54−56] It has also been reported that undulated smectic structure instead of triclinic Sm CG could explain the birefringence along the layer normal.[42] In the present study, observation of bilayer structure using conventional XRD suggests that the triclinic symmetric might indeed exist in the sample. We thus adopt the Sm CG nomenclature and assign the present case as an undulated bilayer $Sm\tilde{C}G_2$ (~ denotes undulation and 2 stands for bilayer). The bilayer structure formation is due to the triclinic symmetry of the bent molecules: eight different possibilities arise while considering both "clinic" and "leaning" of the bent-core molecules, and four of them correspond to bilayer modulation.[55,56]

It is of interest that a relatively larger vinyl substitution group at the 5 position of the central benzene ring leads to an LC phase while the methyl group prohibits the LC behavior. Conjugation between the vinyl group and the central benzene might play an important role in the structure formation. Detailed investigation is ongoing to confirm the LC phase structure and the effect of substitution groups on the mesophase behavior of banana-shaped mesogens. In the following section, we shall focus on the LC mesomorphic behavior of BMJLCPs.

Mesomorphic Properties of the Polymers. (A) Three-Ring BMJLCP System: T-PVCn. Compared to the previously reported PMPCS series, the T-PVC*n* samples possess a 3,5 bent position mesogen linkage instead of the 2,5 linkage; mesogen in T-PVC*n* is thus further away from the backbone. Figure 6 shows the DSC thermograms of T-PVC*n*. Similar to PMPCS, T-PVC*n*s have a glass transition at ~77−133 °C (Table 1), and no first-order transition peaks were observed in the DSC thermograms. PLM experiments showed that this series of samples possess very weak birefringence. Powder WAXD experiments indicated a Φ_N-like diffraction pattern, and Figure 7 shows the WAXD patterns of T-PVC4 at different temperatures. All the diffraction patterns are similar, and they possess a small peak ($d \sim 1.85$ nm) in the low-angle region and an amorphous halo in the wide-angle region. No higher order diffractions were observed in the powder WAXD experiment. However, the packing of the rods could be enhanced by mechanical shear, and Figure 8 shows a 2-D WAXD pattern of sheared T-PVC4. Stronger low-angle diffractions are on the equator, which is the signature of rod formation in the MJLCP WAXD patterns, and the rods are parallel to the shearing

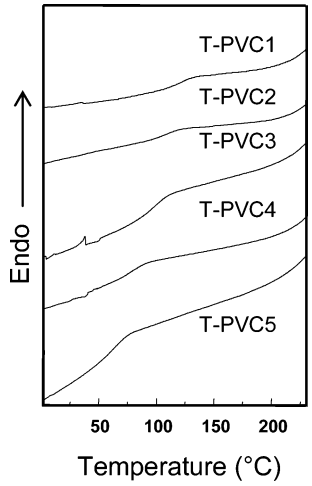

Figure 6. Differential scanning calorimetry thermograms of poly{5-vinyl-1,3-phenylenebis[(4-alkoxy)benzoate]} (T-PVC*n*) at a heating rate of 10 °C/min.

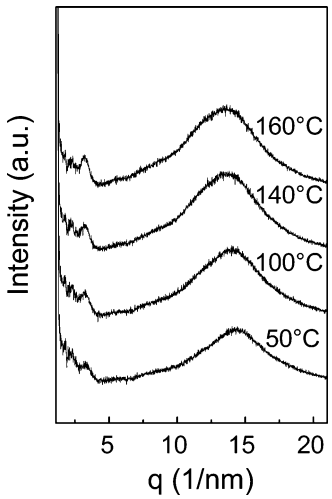

Figure 7. Thermal powder wide-angle X-ray diffraction pattern of poly{5-vinyl-1,3-phenylenebis[(4-butyloxy)benzoate]} (T-PVC4).

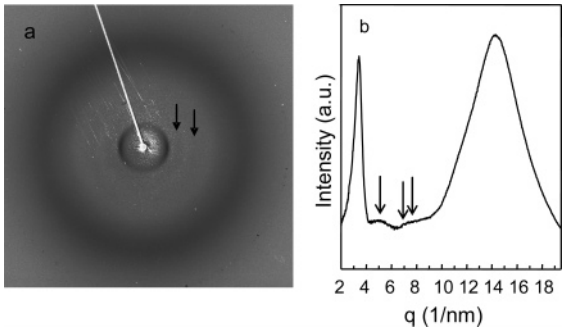

Figure 8. Two-dimensional wide-angle X-ray diffraction pattern of sheared poly{5-vinyl-1,3-phenylenebis[(4-butyloxy)benzoate]} (T-PVC4) (a). Panel b shows the 2θ integration along the equator. Higher order diffractions are evident.

direction. 2θ integration of the 2D pattern (Figure 8b) clearly shows higher order diffractions (arrows), indicating better packing was achieved. These diffraction peaks obey a ratio of 1:1.48:2.16:2.52. Careful analysis shows that it can be assigned as a 2-D lattice, and the diffractions can be indexed as (11), (20), (13), and (04). The rectangular lattice can therefore be calculated as $a = 2.50$ nm and $b = 2.76$ nm, and the LC phase can thus be assigned as a columnar rectangular phase (Φ_R). Observation of rectangular packing of the LC rods is of interest.

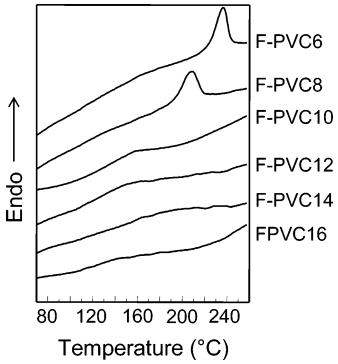

Figure 9. Differential scanning calorimetry thermograms of poly{5-vinyl-1,3-phenylenebis[4-(4′-alkoxybenzoyloxy)benzoate]} [F-PVC*n*, (*n* = 6−16)] at the heating rate of 40 °C/min.

The Φ_R phase has been reported in self-assembled dendrons by Percec et al.[25,26] Both primitive *P*2*mm* and centered *C*2*mm* two-dimensional lattices were proposed. Our observation fits the *C*2*mm* lattice, and we shall return to Φ_R phase packing of the BMJLCP in the following section.

Compared to the previously reported PMPCS, it is evident that by changing the mesogenic substituting group from the 2,5 position to the 3,5 position, the LC ordering changed. The relatively broad diffraction peaks indicate that the rod structure in the present case might not be as uniform as those formed by PMPCS. We envisage that, in the 3,5 mesogen jacketing, the interaction between the backbone and the mesogen groups is not as close as that in the 2,5 mesogen systems. Polymer backbones, therefore, possess more "free volume" for segmental motion and the "jacketing effect" is weakened. Polymer rods formed in such systems may not be uniform. This observation also demonstrated that "close jacketing" between the side-chain mesogen and the polymer backbone is essential to the LC phase formation in the MJLCP systems.

(B) Five-Ring BMJLCP System: F-PVC*n*. To increase the steric hindrance between the side chain and the polymer backbone in the MJLCP system, one way is to vary the linkage position of the backbone to the mesogen. The other possible approach is to increase the size of the side groups (Scheme 1d). Larger side groups impose stronger steric hindrance, and a nearly extended chain could be achieved. To investigate the size effect, five-ring BMJLCPs were synthesized as summarized in Table 1. TGA analysis shows that all of these polymers are stable until ∼300 °C. Figure 9 shows the DSC thermograms of F-PVC*n*. By using a relatively large amount of sample and fast heating following slow cooling, the T_g is detectable at ∼114−140 °C for F-PVC*n* samples. DSC thermograms of F-PVC6 and -8 show a glass transition as well as an endothermic peak at 210−240 °C, while, in samples F-PVC10−16, only the glass transition was observed, indicating that the LC state is stable until thermal degradation in these samples. F-PVC6 and -8 showed a first-order transition upon heating, while the others did not. A possible reason might be that the macromolecular column packing is not perfectly achieved (see the following discussion) due to the short tails in F-PVC6 and -8. PLM experiments show that F-PVC-6, -8, -10, and -12 are weakly birefringent, while F-PVC14 and -16 possess relatively strong birefringence (Figure 10). LC Schlieren texture was formed when the sample was heated to 180 °C. Upon further heating, no visual disappearance of birefringence could be observed before the polymer decomposition. When cooled to room temperature from 300 °C, the birefringence of the sample was retained, indicating that the ordered structure formed at high temperature was maintained upon cooling. LC structures were

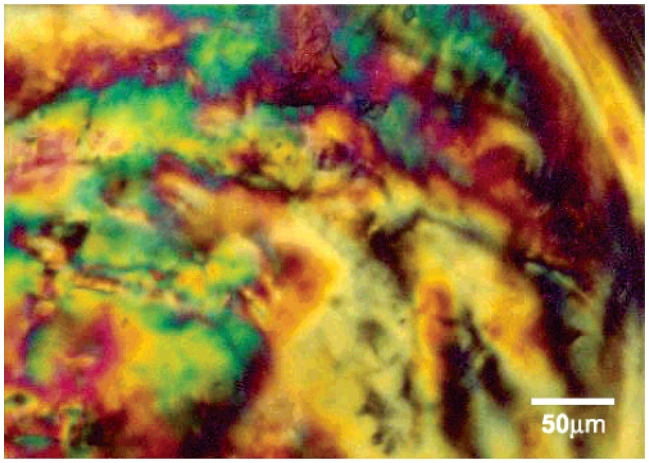

Figure 10. Polarized light microscope image shows the Schlieren texture of poly{5-vinyl-1,3-phenylenebis[4-(4′-tetradecyloxybenzoyloxy)benzoate]} (F-PVC14).

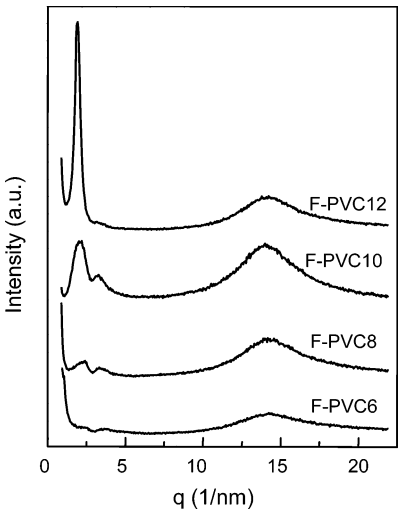

Figure 11. Powder wide-angle X-ray diffraction pattern of poly{5-vinyl-1,3-phenylenebis[4-(4′-alkoxybenzoyloxy)benzoate]} [F-PVC*n* (*n* = 6−12)].

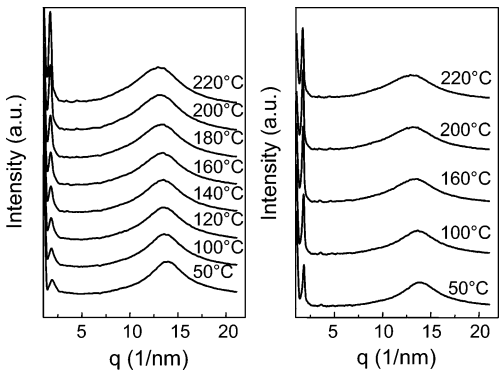

Figure 12. Thermal powder wide-angle X-ray diffraction of poly{5-vinyl-1,3-phenylenebis[4-(4′-tetradecyloxybenzoyloxy)benzoate]} (F-PVC14).

confirmed by WAXD, and Figure 11 shows the powder WAXD of F-PVC6−12. The diffraction patterns of F-PVC6 and -8 are evidently different from F-PVC10 and -12, consistent with the DSC data. In F-PVC6 and -8, the low-angle diffraction peaks are weak while the diffraction intensity dramatically increases as the tail length increases (diffraction patterns of F-PVC14 and -16 are similar to that of F-PVC12, as shown in Figure 12). Also, for the low-angle diffraction peak, F-PCV6−10 show

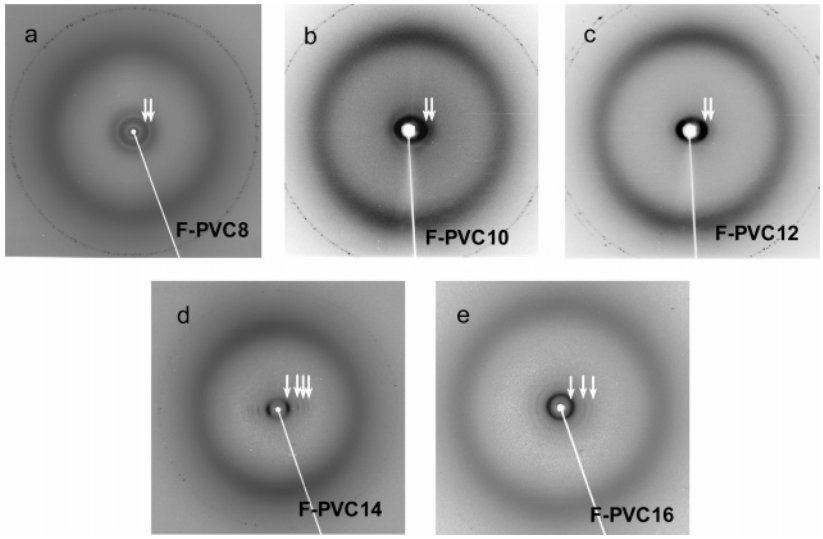

Figure 13. Two-dimensional wide-angle X-ray diffraction pattern of sheared poly{5-vinyl-1,3-phenylenebis[4-(4′-alkoxybenzoyloxy)benzoate]} (F-PVC*n*), where n = (a) 8, (b) 10, (c) 12, (d) 14, and (e) 16.

Table 2. Liquid Crystalline (LC) Strucutres and Lattice Parameters of Poly{5-vinyl-1,3-phenylenebis[4-(4′-alkoxybenzoyloxy)benzoate]} (F-PVC*n*)

polymer[a]	diffraction q [b] (obsd, nm^{-1})	LC phase	lattice params (nm)
F-PVC8	2.09, 3.28	Φ_R	$a = 3.83$, $b = 4.83$
F-PVC10	1.91, 2.77	Φ_R	$a = 4.53$, $b = 4.79$
F-PVC12 (as sheared)	1.86, 2.94	Φ_R	$a = 4.27$, $b = 5.51$
F-PVC12 (annealed)	1.88, 3.26, 3.77, 4.21, 4.97, 5.67	Φ_H	$a = 3.89$
F-PVC14	1.77, 3.05 3.54, 4.64, 5.31	Φ_H	$a = 4.09$
F-PVC16	1.73, 2.92, 3.43, 4.53	Φ_H	$a = 4.29$

[a] As defined in Scheme 2b. [b] Measured using two-dimensional wide-angle X-ray experiments.

larger full width at half-height, while the diffraction becomes much sharper for F-PVC12−16, suggesting better ordered structure was formed as the LC tail length increases.

Figure 12 shows the thermal WAXD results of F-PVC14 during a heating/cooling scan at a rate of 10 °C/min. In both heating and cooling curves, the wide-angle scattering halo remained unchanged, suggesting no long-range-ordered structure was formed via molecular packing on a scale of about 0.5 nm over the entire temperature region examined. The intensity of the low-angle peak substantially increased upon heating and slightly decreased during the subsequent cooling. The *d*-spacing obtained from XRD varied from 3.3 to 3.7 nm at different temperatures. Higher order diffractions became evident after the temperature reached 160 °C, and the structure was retained during cooling.

To further characterize the mesomorphic phase behavior, 2-D WAXD experiments were conducted. Polymer film was mechanically sheared at ∼200 °C in order to achieve chain orientation. Parts a−e of Figure 13 show the 2-D XRD pattern of F-PVC8, -10, -12, -14, and -16. Shear direction is parallel to the meridian in each of the diffraction patterns. The diffraction patterns are similar to those of other MJLCP systems: The low-angle diffraction peak suggests the formation of macromolecular columns. In the case of the F-PVC*n* system, the *d* spacing can be found to be 3.00, 3.28, 3.37, 3.54, and 3.62 nm for F- PVC8, -10, -12, -14, and -16, respectively (Table 2). Observing these arcs on the equator of the XRD pattern and the rectangular relationship between the low- and wide-angle scatterings suggests that the macromolecular columns are aligned parallel to the shear direction, a feature that is commonly observed in all MJLCP systems.

Careful study of the 2-D pattern along the equator direction shows that in F-PVC6, the low-angle reflection is not clear (consistent with the 1-D WAXD data, not shown) while in PFVC8, -10, -12, -14, and -16, higher order diffractions can be clearly seen. The ratios of these diffractions with respect to the first strong diffraction are different, as shown in Table 2. For F-PVC8, -10, and -12, two peaks appear at q =2.09 and 3.28 nm^{-1} (1:1.57); 1.91 and 2.77 nm^{-1} (1:1.45); and 1.86 and 2.94 nm^{-1} (1:1.58), respectively. For F-PVC14 and -16, up to four diffraction peaks can be observed, and detailed analysis shows that F-PVC14−16 exhibit higher order diffractions with the ratio of $1{:}\sqrt{3}{:}\sqrt{4}{:}\sqrt{7}$, indicating a hexagonal packing and the corresponding LC phase is Φ_H. In F-PVC8−12, however, the packing does not obey the hexagonal order. Due to the lack of higher order diffractions, the packing scheme cannot be unambiguously resolved. Since the ratios of the first two diffraction peaks of F-PVC10−12 are similar to that of T-PVC4, rectangular packing of the rods might occur and the corresponding phase is Φ_R. Similar to T-PVC4, the first two diffraction peaks can be assigned as (11) and (20) and the corresponding lattice parameters are listed in Table 2. To obtain better packing, the sheared samples were further annealed at 180 °C for 12 h and diffraction patterns of F-PVC10, -14, and -16 did not change except for intensity enhancement. In contrast, the diffraction pattern of F-PVC12 dramatically changed, as shown in Figure 14. Six diffraction arcs, which also obey the $1{:}\sqrt{3}{:}\sqrt{4}{:}\sqrt{5}{:}\sqrt{7}{:}\sqrt{9}$ ratio as shown by the 2θ integration of the WAXD pattern along the equator, indicate that by annealing, the packing changed from the possible rectangular to hexagonal order.

Two columnar packing schemes were observed in F-PVC*n*. It is envisaged that this difference in packing schemes might be due to the "softness" of the macromolecular rod surface, as shown in Figure 15. In small mass liquid crystals, introduction of shape biaxiality of the mesogen has led to an optically biaxial nematic (N_b) phase.[57−60] Both laterally attached LCP and a

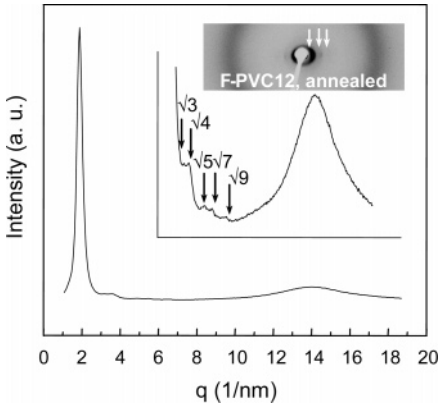

Figure 14. 2θ integration of the wide-angle X-ray diffraction pattern along equator of the annealed poly{5-vinyl-1,3-phenylenebis[4-(4′-dodecyloxybenzoyloxy)benzoate]} (F-PVC12) sample. Hexagonal packing can be clearly seen. Inset shows the equator section of the two-dimensional diffraction pattern.

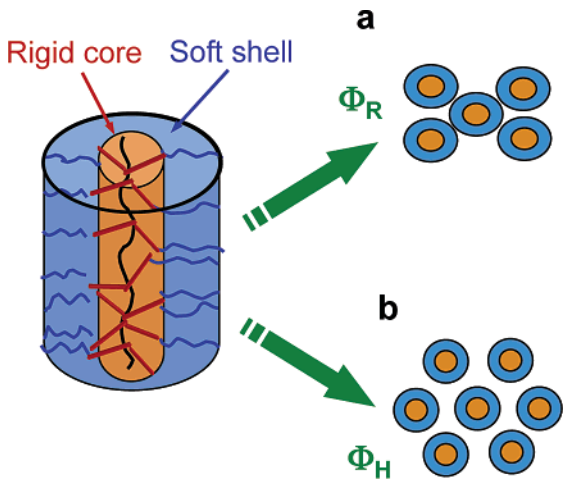

Figure 15. Schematic representation of (a) columnar rectangular (Φ_R) and (b) columnar hexagonal (Φ_H) phases.

cyanobiphenyl-coupled BCLC showed this unique phase behavior. In the present case, due to the shape biaxiality of BCLC, in short-tail homologues, the macromolecular columns formed by the BMJLCPs might not be uniaxial from the simple geometry point of view, leading to the Φ_R phase. As the tail length increases, the surface of the rods are covered with more aliphatic chains, which are "soft" and better packing can therefore be obtained. This Φ_R phase also resembles N_b on the supramolecular/macromolecular scale. Detailed phase structure is currently under investigation.

Conclusions

In summary, a series of novel BMJLCPs were synthesized. A mesomorphic phase was not observed in any of the three-ring bent-core monomers. Sm$\tilde{C}G_2$ was, for the first time, observed in the 5-substituted five-ring bent-core system in monomers with relatively longer tails (F-VC14 and F-VC16). The Φ_R phase was, for the first time, observed in MJLCP systems. BMJLCPs with three bent-core rings show this novel phase behavior, while two different columnar phases, Φ_R and Φ_H, were observed in the five-ring system. The phase formation was found to be critically dependent on the aliphatic tail length: F-PVC8 and -10 showed a possible Φ_R behavior. F-PVC14 and -16 exhibited a uniform hexagonal order. The different packing orders in F-PVC*n* may be due to the surface "softness" of the macromolecular rod: as the tail length increases, better packing could be achieved. Since the *n*-alkoxy substituent lengths for the three-ring and five-ring were different, detailed comparison of the LC phase behaviors between the three-ring and five-ring systems with similar *n*-alkoxy tail lengths will be conducted in the future investigation. This novel BMJLCP provides a unique opportunity to investigate rod−coil systems with tunable rod structures.

Acknowledgment. This work was supported by the National Natural Science Foundation of China (Grant 20134010), the National Science Foundation (NSF CAREER Award, DMR-0239415), the donors of the ACS Petroleum Research Fund, 3M, and DuPont. X.C. is thankful for the support from the Doctoral Program of the Higher Education Institution of the Ministry of Education (Grant 20030001061). We thank Steven Ehrlich, Igors Sics, and Prof. Benjamin H. Hsiao for help with the X-ray experiments at beam lines X-18A and X-27C in the National Synchrotron Light Source, Brookhaven National Laboratory. C.Y.L. thanks the Mettler-Toledo Co. for the Turi award supporting the thermal analysis equipment purchase.

References and Notes

(1) Allegra, G.; Meille, S. V. *Macromolecules* **2004**, *37*, 3487−3496.
(2) Zhou, Q. F. L.; H. M.; Feng, X. D. *Macromolecules* **1987**, *20*, 233−234.
(3) Zhou, Q. F.; Wan, X. H.; Zhu, X. L.; Zhang, F.; Feng, X. D. *Mol. Cryst. Liq. Cryst.* **1993**, *231*, 107−117.
(4) Hardouin, F.; Mery, S.; Achard, M. F.; Noirez, L.; Keller, P. *J. Phys. II* **1991**, *1*, 511−520.
(5) Hardouin, F.; Leroux, N.; Mery, S.; Noirez, L. *J. Phys. II* **1992**, *2*, 271−278.
(6) Zhou, Q. F. Z.; X. L.; Wen. Z. Q. *Macromolecules* **1989**, *22*, 491−493.
(7) Pragliola, S.; Ober, C. K.; Mather, P. T.; Jeon, H. G. *Macromol. Chem. Phys.* **1999**, *200*, 2338−2344.
(8) Zhang, D.; Zhou, Q. F.; Ma, Y. G.; Wan, X. H.; Feng, X. D. *Polym. Adv. Technol.* **1997**, *8*, 227−233.
(9) Zhang, D.; Liu, Y. X.; Wan, X. H.; Zhou, Q. F. *Macromolecules* **1999**, *32*, 5183−5185.
(10) Yu, Z. N.; Tu, H. L.; Wan, X. H.; Chen, X. F.; Zhou, Q. F. *J. Polym. Sci. Polym. Chem.* **2003**, *41*, 1454−1464.
(11) Li, C. Y.; Tenneti, K. K.; Zhang, D.; Zhang, H. L.; Wan, X. H.; Chen, E. Q.; Zhou, Q. F.; Avila-Orta, C.; Igos, S.; Hsiao, B. S. *Macromolecules* **2004**, *37*, 2854−2860.
(12) Ye, C.; Zhang, H. L.; Huang, Y.; Chen, E. Q.; Lu, Y. L.; Shen, D. Y.; Wan, X. H.; Shen, Z. H.; Cheng, S. Z. D.; Zhou, Q. F. *Macromolecules* **2004**, *37*, 7188−7196.
(13) Tu, H. L.; Wan, X. H.; Liu, Y. X.; Chen, X. F.; Zhang, D.; Zhou, Q. F.; Shen, Z. H.; Ge, J. J.; Jin, S.; Cheng, S. Z. D. *Macromolecules* **2000**, *33*, 6315−6320.
(14) Yin, X. Y.; Ye, C.; Ma, X.; Chen, E. Q.; Qi, X. Y.; Duan, X. F.; Wan, X. H.; Cheng, S. Z. D.; Zhou, Q. F. *J. Am. Chem. Soc.* **2003**, *125*, 6854−6855.
(15) Wan, X. H.; Tu, H. L.; Tu, Y. F.; Zhang, D.; Sun, L.; Zhou, Q. F.; Dong, Y. P.; Tang, M. *Chin. J. Polym. Sci.* **1999**, *17*, 189−192.
(16) Zhang, H.; Yu, Z.; Wan, X.; Zhou, Q. F.; Woo, E. M. *Polymer* **2002**, *43*, 2357−2361.
(17) Lecommandoux, S.; Noirez, L.; Achard, M. F.; Hardouin, F. *Macromolecules* **2000**, *33*, 67−72.
(18) Lecommandoux, S.; Hardouin, F.; Dianoux, A. J. *Eur. Phys. J. B* **1998**, *5*, 79−85.
(19) Kim, G. H.; Pugh, C.; Cheng, S. Z. D. *Macromolecules* **2000**, *33*, 8983−8991.
(20) Arehart, S. V.; Pugh, C. *J. Am. Chem. Soc.* **1997**, *119*, 3027−3037.
(21) Pugh, C.; Bae, J. Y.; Dharia, J.; Ge, J. J.; Cheng, S. Z. D. *Macromolecules* **1998**, *31*, 5188−5200.
(22) Small, A. C.; Pugh, C. *Macromolecules* **2002**, *35*, 2105−2115.
(23) Gopalan, P.; Andruzzi, L.; Li, X. F.; Ober, C. K. *Macromol. Chem. Phys.* **2002**, *203*, 1573−1583.
(24) Percec, V.; Ahn, C. H.; Ungar, G.; Yeardley, D. J. P.; Moller, M.; Sheiko, S. S. *Nature* **1998**, *391*, 161−164.
(25) Percec, V.; Glodde, M.; Bera, T. K.; Miura, Y.; Shiyanovskaya, I.; Singer, K. D.; Balagurusamy, V. S. K.; Heiney, P. A.; Schnell, I.; Rapp, A.; Spiess, H. W.; Hudson, S. D.; Duan, H. *Nature* **2002**, *419*, 384−387.

(26) Percec, V.; Mitchell, C. M.; Cho, W. D.; Uchida, S.; Glodde, M.; Ungar, G.; Zeng, X. B.; Liu, Y. S.; Balagurusamy, V. S. K.; Heiney, P. A. *J. Am. Chem. Soc.* **2004**, *126*, 6078−6094.
(27) Gopalan, P.; Zhang, Y. M.; Li, X. F.; Wiesner, U.; Ober, C. K. *Macromolecules* **2003**, *36*, 3357−3364.
(28) Wan, X. H.; Tu, Y. F.; Zhang, D.; Zhou, Q. F. *Polym. Int.* **2000**, *49*, 243−247.
(29) Zhang, H. L.; Tu, Y. F.; Wan, X. H.; Zhou, Q. F.; Woo, E. M. *J. Polym. Res.* **2002**, *9*, 11−15.
(30) Yi, Y.; Wan, X. H.; Fan, X. H.; Dong, R.; Zhou, Q. F. *J. Polym. Sci., Part A: Polym. Chem.* **2003**, *41*, 1799−1806.
(31) Zhang, H. L.; Chen, X. F.; Wan, X. H.; Zhou, Q. F.; Woo, E. M. *Polym. Int.* **2003**, *52*, 92−97.
(32) Yi, Y.; Fan, X. H.; Wan, X. H.; Li, L.; Zhao, N.; Chen, X. F.; Xu, J.; Zhou, Q. F. *Macromolecules* **2004**, *37*, 7610−7618.
(33) Tu, Y. F.; Wan, X. H.; Zhang, D.; Zhou, Q. F.; Wu, C. *J. Am. Chem. Soc.* **2000**, *122*, 10201−10205.
(34) Tu, Y. F.; Wan, X. H.; Zhang, H. L.; Fan, X. H.; Lu, D. N.; Chen, X. F.; Zhou, Q. F. *Chin. J. Polym. Sci.* **2003**, *21*, 569−573.
(35) Tu, Y. F.; Wan, X. H.; Zhang, H. L.; Fan, X. H.; Chen, X. F.; Zhou, Q. F.; Chau, K. C. *Macromolecules* **2003**, *36*, 6565−6569.
(36) Vorländer, D. *Z. Phys. Chem.* **1923**, *105*, 211−254.
(37) Niori, T. S. T.; Watanabe, J. et al. *J. Mater. Chem.* **1996**, *6*, 1231−1233.
(38) Sekine, T.; Takanishi, Y.; Niori, T.; Watanabe, J.; Takezoe, H. *Jpn. J. Appl. Phys., Part 2* **1997**, *36*, L1201−L1203.
(39) Pelzl, G.; Wirth, I.; Weissflog, W. *Liq. Cryst.* **2001**, *28*, 969−972.
(40) Choi, S. W.; Kinoshita, Y.; Park, B.; Takezoe, H.; Niori, T.; Watanabe, J. *Jpn. J. Appl. Phys.* **1998**, *37*, 3408−3411.
(41) Link, D. R.; Natale, G.; Shao, R.; Maclennan, J. E.; Clark, N. A.; Korblova, E.; Walba, D. M. *Science* **1997**, *278*, 1924−1927.
(42) Shen, D.; Diele, S.; Wirt, I.; Tschierske, C. *Chem. Commun.* **1998**, 2573−2574.
(43) Pelzl, G.; Diele, S.; Weissflog, W. *Adv. Mater.* **1999**, *11*, 707−724.
(44) Walba, D. M.; Korblova, E.; Shao, R.; Maclennan, J. E.; Link, D. R.; Glaser, M. A.; Clark, N. A. *Science* **2000**, *288*, 2181−2184.
(45) Keith, C.; Reddy, R. A.; Tschierske, C. *Chem. Commun.* **2005**, 871−873.
(46) Sentman, A. C.; Gin, D. L. *Angew. Chem., Int. Ed.* **2003**, *42*, 1815−1819.
(47) Barbera, J.; Gimeno, N.; Monreal, L.; Pinol, R.; Ros, M. B.; Serrano, J. L. *J. Am. Chem. Soc.* **2004**, *126*, 7190−7191.
(48) Fodor-Csorba, K.; Vajda, A.; Galli, G.; Jakli, A.; Demus, D.; Holly, S.; Gacs-Baitz, E. *Macromol. Chem. Phys.* **2002**, *203*, 1556−1563.
(49) Weissflog, W.; Nadasi, H.; Dunemann, U.; Pelzl, G.; Diele, S.; Eremin, A.; Kresse, H. *J. Mater. Chem.* **2001**, *11*, 2748−2758.
(50) Reddy, R. A.; Sadashiva, B. K. *Liq. Cryst.* **2004**, *31*, 1069−1081.
(51) Schroder, M. W.; Diele, S.; Pelzl, G.; Weissflog, W. *ChemPhysChem* **2004**, *5*, 99−103.
(52) Coleman, D. A.; Fernsler, J.; Chattham, N.; Nakata, M.; Takanishi, Y.; Korblova, E.; Link, D. R.; Shao, R. F.; Jang, W. G.; Maclennan, J. E.; Mondainn-Monval, O.; Boyer, C.; Weissflog, W.; Pelzl, G.; Chien, L. C.; Zasadzinski, J.; Watanabe, J.; Walba, D. M.; Takezoe, H.; Clark, N. A. *Science* **2003**, *301*, 1204−1211.
(53) Bedel, J. P.; Rouillon, J. C.; Marcerou, J. P.; Nguyen, H. T.; Achard, M. F. *Phys. Rev. E* **2004**, *69*.
(54) de Gennes, P. G. *The Physics of Liquid Crystals*; Chlarendon Press: Oxford, U.K., 1975.
(55) Brand, H. R.; Cladis, P. E.; Pleiner, H. *Eur. Phys. J. B* **1998**, *6*, 347−353.
(56) Jakli, A.; Kruerke, D.; Sawade, H.; Heppke, G. *Phys. Rev. Lett.* **2001**, *86*, 5715−5718.
(57) Hegmann, T.; Kain, J.; Diele, S.; Pelzl, G.; Tschierske, C. *Angew. Chem., Int. Ed.* **2001**, *40*, 887−890.
(58) Hessel, F.; Finkelmann, H. *Polym. Bull.* **1986**, *15*, 349−352.
(59) Hunt, J. J.; Date, R. W.; Timimi, B. A.; Luckhurst, G. R.; Bruce, D. W. *J. Am. Chem. Soc.* **2001**, *123*, 10115−10116.
(60) Yu, L. J.; Saupe, A. *Phys. Rev. Lett.* **1980**, *45*, 1000−1003.

MA051939D